A geometrical approach to wave-type solutions of excitable reaction–diffusion systems

By P. Grindrod†, M. A. Lewis‡ and J. D. Murray‡

Centre for Mathematical Biology, Mathematical Institute, 24–29 St Giles', Oxford OX1 3LB, U.K.

We formulate the eikonal equation approximation for travelling waves in excitable reaction–diffusion systems, which have been proposed as models for a large number of biomedical situations. This formulation is particularly suited, in a natural way, to numerical solution by finite difference methods. We show how this solution is independent of the parametric variable used for expressing the eikonal equation, and how a reduction of dimensionality implies a major saving over the time taken to solve the original reaction–diffusion system. Neumann boundary conditions on reactants in the original system translate into a geometric constraint on the wave boundary itself. We show how this leads to geometrically stable stationary wave boundaries in appropriately shaped non-convex domains. This analytical prediction is verified by numerical solution of the eikonal equation on a domain which supports geometrically stable stationary wave boundary configurations. We show how the concepts of geometrical stability and wave-front stability relate to a problem where a bi-stable reaction–diffusion system has a stable stationary wave-front configuration.

1. Introduction

Much analytical research into reaction–diffusion systems is concerned with their plane wave solutions (see, for example, Murray 1989). Even for small systems, the existence and stability problems for these travelling waves are challenging. In this paper, we shall consider three-dimensional waves that propagate over surfaces which do not necessarily have planar symmetry.

A plane travelling wave front has constant velocity at all points in the forward, normal direction. If the plane geometry of the wave is distorted, the normal velocity will now vary locally across the wave front.

As background we need a general idea as to what constitutes a wave or wave-like structure. We shall use these terms to refer to solutions which cause the state of the system to be changed qualitatively and successively in adjacent neighbourhoods in the domain. For example, a wave-front changes the state of the system from one steady state to another as it passes over. By choosing an intermediate state, we can define a surface of points in the domain at which this specific state is obtained. As time evolves, the progress of this surface represents the progress of the wave-front,

† Present address: Intera-Sciences (Environmental Sciences Department), Chiltern House, 45 Station Road, Henley-on-Thames, Oxfordshire RG9 1AT, U.K.

‡ Present address: Department of Applied Maths FS-20, and Department of Zoology NJ-15, University of Washington, Seattle, Washington 98195, U.S.A.

Proc. R. Soc. Lond. A (1991) **433**, 151–164
Printed in Great Britain

and the normal velocity and curvature of this surface will vary with space and time. Of course, had we chosen an alternative intermediate state, we would have obtained a different surface, probably propagating according to slightly different rules. A full knowledge of the behaviour of each and every such surface would require a complete knowledge of the solution to the original reaction–diffusion problem.

We now wish to exploit the notion of a surface of points, representing the location of a wave-front, in our analysis. We do this by restricting the nature of the systems that are under consideration. Specifically, we consider those systems with excitable dynamics. These systems possess a fast variable which dominates the behaviour of the system. Small subthreshold perturbations of this fast variable from the unique steady state are rapidly damped out, but larger suprathreshold perturbations trigger an abrupt and substantial wave-like excursion from the steady state to an excited state, after which there is an eventual return to the steady state. This excursion is characterized by a transition-layer or wave boundary in which the dominant variable shifts rapidly from the steady state to the excited state. This leads to two major analytical advantages.

First, it suggests that we try to solve the problems by a transition-layer approach, which often proves successful for problems involving travelling waves. As it turns out, it is the behaviour of the solution within the transition-layer that is important in describing the spreading of the wave.

Secondly, since the state is changing rapidly across the transition-layer, the surfaces at which the solution achieves specific intermediate states are all very close together, and hence must exhibit a similar geometry and normal speed of propagation. Thus we avoid the complexities involved in the general situation indicated earlier.

Assuming that the waves are quiescent away from the transition layers, the problem reduces to the following: to describe how the solution varies across the transition-layer, and to describe how the geometry and motion of the transition-layer (wave boundary) evolves in time.

A number of authors, including Zykov (see, for example, Zykov 1987), Keener & Tyson (see, for example, Keener 1986; Keener & Tyson 1986) have shown how wave boundary motion depends crucially upon its curvature. Following Gomatam & Grindrod (1987), we indicate how the problem of two- and three-dimensional wave propagation can be compared with that for wave propagation in one dimension by requiring that the wave boundary is located on a surface which propagates according to

$$N+\epsilon\kappa = c,$$

where N is normal velocity, κ is twice the mean curvature, and ϵ and c are constants obtained independently from the original reaction–diffusion equation. We refer to this as the eikonal equation (see Keener 1986).

We shall show that solutions to the eikonal equation exhibit stability and threshold behaviours which are analogous to the same concepts when applied to the original reaction diffusion system. That such behaviour has been inherited by the eikonal equation suggests the fundamental nature of the eikonal equation as a model for solutions of reaction–diffusion systems.

If a wave is in contact with a boundary (that is, a boundary of the domain of the original reaction–diffusion system), we impose boundary conditions which are consistent with Neumann boundary conditions for the original reaction–diffusion system. For a wave meeting the boundary, this simply requires that the edge of the wave-front must propagate so that the wave always meets the boundary orthogonally (that is, the normal vectors to the surface locating the wave front and the boundary surface are orthogonal).

We shall show how the application of orthogonal boundary conditions to the eikonal equation may result in stable stationary solutions as a wave exits, for example, from a narrow slit into a larger reservoir (see also Grindrod 1991). This is used to give a simple explanation of the result that homogenous reaction–diffusion systems with two or more stable rest states possess stable non-homogenous steady state solutions in certain non-convex domains. The classic example is a steady state solution in a dumb-bell shaped region, a narrow bridge between two large convex sub-domains (Matano 1979). Here, the bridge is a small slit in our present terminology. We shall show that, even though plane waves propagate down the slit, changing the system from one rest state to another, they can cap the slit at one end by a circular arc which is a stable stationary configuration.

The main motivation for studying excitable reaction–diffusion equations lies in their applicability to problems in physiology, biology and chemistry (Murray 1989). Excitable behaviour is typically exhibited by nerve axons (Hodgkin & Huxley 1952; FitzHugh 1961; Nagumo *et al.* 1962), neuromuscular tissues (Winfree 1987; Shibata & Bŭres 1974; Gorelova & Bŭres 1983; Muira & Plant 1981; Lewis & Grindrod 1991), select chemical reactions in non-convecting liquid phase, such as the Belousov–Zhabotinskii reaction (Keener & Tyson 1986) and some biological aggregates such as slime molds (Tyson *et al.* 1989; Tyson & Murray 1989). For example, the Hodgkin–Huxley equations provide an important model for the electrical activity in membranes of living organisms. One of the state variables represents the potential difference across the membrane. This is subject to the electrical currents conducted tangentially to the membrane in both the external and internal ionic fluids, as well as trans-membrane currents due to the gating of specific charged ions through active channels, as well as the capacitance of the membrane itself. In one dimension, the Hodgkin–Huxley equations are used as a model for the propagation of action potentials along an unmyelinated nerve axon: this was the original problem for which the equations were derived (Hodgkin & Huxley 1952). The FitzHugh–Nagumo (FitzHugh 1961; Nagumo *et al.* 1962) equations constitute a similar, but more qualitative, model.

Our aim is to use the eikonal equation approximation to investigate analytically and numerically the behaviour of wave boundaries on two-dimensional surfaces. In §2 we formulate the eikonal equation approximation in a parametric form and show how, in certain instances, the parametric variables can be dispensed with. In §3 we introduce a simplified time evolution equation for the movement of waves on two-dimensional surfaces. In §4 we show that, in fact, this equation can be solved numerically, even though it is expressed in a parametric form. This is a new result, and is significant in that it yields a remarkable computational advantage over solving the original reaction–diffusion system. In §5 we predict the configurations and geometric stabilities of waves passing through narrow slits. Here the wave boundaries are constrained to be highly curved due to the combined effects of the boundary conditions and domain geometry present in the original reaction–diffusion system.

2. The eikonal equation

We consider the excitable reaction–diffusion system

$$u_t = D_1 \Delta u + f(u, v), \quad v_t = D_2 \Delta v + \epsilon g(u, v), \tag{1}$$

where t is time, Δ is the laplacian operator with respect to the space vector $\boldsymbol{x} \in \mathbb{R}^3$, f and g define the excitable reaction kinetics and $0 < \epsilon \ll 1$. Here u is the 'fast' variable and v is the 'slow' variable. By rescaling

$$\boldsymbol{x} \to \epsilon \boldsymbol{x}/D_1^{\frac{1}{2}}, \quad t \to \epsilon t, \quad \delta \to D_2/D_1$$

we change (1) to a form suitable for our analysis:

$$\epsilon u_t = \epsilon^2 \Delta u + f(u, v), \quad v_t = \epsilon\delta\Delta v + g(u, v). \tag{2}$$

We introduce the moving coordinate system

$$\boldsymbol{r} = \boldsymbol{r}(\mu, \eta, \lambda, t),$$

where $\{\mu, \eta, \lambda\}$ constitutes a triply orthogonal system of coordinates

$$\boldsymbol{r}_\mu \cdot \boldsymbol{r}_\lambda = 0, \quad \boldsymbol{r}_\lambda \cdot \boldsymbol{r}_\eta = 0, \quad \boldsymbol{r}_\eta \cdot \boldsymbol{r}_\mu = 0, \quad |\boldsymbol{r}_\mu| = 1,$$

$\boldsymbol{r}_\mu = \partial \boldsymbol{r}/\partial\mu$ and similarly for $\boldsymbol{r}_\lambda$ and $\boldsymbol{r}_\eta$. At any time, t, the surface given by $\boldsymbol{r}(0, \eta, \lambda, t)$ is the wave boundary, or wave-front boundary layer, parametrized by η and λ. Thus

$$\boldsymbol{r}_\mu = \frac{\boldsymbol{r}_\eta \times \boldsymbol{r}_\lambda}{|\boldsymbol{r}_\eta|\,|\boldsymbol{r}_\lambda|} \tag{3}$$

is the unit vector normal to the wave boundary, and

$$\boldsymbol{r}_t = N\boldsymbol{r}_\mu, \tag{4}$$

where N is the normal velocity of the wave boundary.

Following the procedure in Gomatam & Grindrod (1987), we use the stretched coordinate $\xi = \mu/\epsilon$ to find solutions for the fast variable of the form $u = U(\xi)$, and arrive at an asymptotic approximation for N in terms of the one-dimensional travelling wave speed, denoted by c, and twice the mean curvature of the wave boundary, denoted by κ. This approximation, given by

$$N = c - \epsilon\kappa, \tag{5}$$

where
$$\kappa = -\frac{\boldsymbol{r}_{\eta\eta} \cdot (\boldsymbol{r}_\eta \times \boldsymbol{r}_\lambda)}{|\boldsymbol{r}_\eta|^3 |\boldsymbol{r}_\lambda|} - \frac{\boldsymbol{r}_{\lambda\lambda} \cdot (\boldsymbol{r}_\eta \times \boldsymbol{r}_\lambda)}{|\boldsymbol{r}_\eta|\,|\boldsymbol{r}_\lambda|^3}, \tag{6}$$

is referred to as the eikonal equation for reaction diffusion systems and is valid to $O(\epsilon)$. Thus (3), (4), (5) and (6) describe the time evolution of the wave boundary.

If the wave boundary $\boldsymbol{r}(0, \eta, \lambda, t)$ can be expressed as a single-valued function, then the dummy coordinates η and λ can be dispensed with. For example, if the wave boundary can be written in the form $x = x(\eta, \lambda, t) = X(y, z, t)$, then the time evolution equation becomes

$$X_t = c(1 + X_y^2 + X_x^2)^{\frac{1}{2}} + \epsilon\left(\frac{X_{yy}(X_z^2+1) - 2X_{yz}X_yX_z + X_{zz}(X_y^2+1)}{1 + X_y^2 + X_z^2}\right). \tag{7}$$

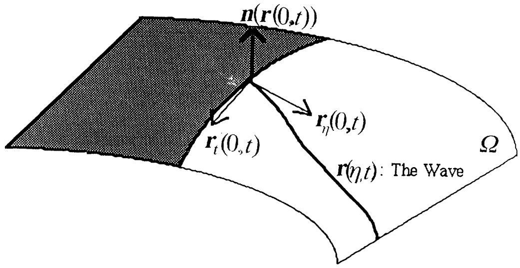

Figure 1. The wave meets $\partial\Omega$ in S. Zero-flux boundary conditions constrain $\boldsymbol{r}_\eta$ to be perpendicular to $\partial\Omega$.

3. Waves on two-dimensional surfaces

If we restrict our attention to waves propagating over some oriented smooth surface, S, we can choose $\boldsymbol{r}^* \in S$ and $\boldsymbol{n}(\boldsymbol{r}^*)$ to be the oriented unit normal to S and set

$$\boldsymbol{r} = \boldsymbol{r}^*(\eta, t) + \lambda \boldsymbol{n}(\boldsymbol{r}^*(\eta, t)).$$

This is equivalent to seeking three-dimensional waves that intersect S orthogonally along $\boldsymbol{r}^*(\eta, t)$. The time evolution of the wave boundary, given by (3), (4), (5) and (6), now simplifies to yield an equation for the propagation of waves on the surface S, namely

$$\boldsymbol{r}_t = (c - \epsilon\kappa)\frac{\boldsymbol{r}_\eta \times \boldsymbol{n}}{|\boldsymbol{r}_\eta|} = \left(c + \epsilon\frac{\boldsymbol{r}_{\eta\eta}\cdot\boldsymbol{r}_\eta \times \boldsymbol{n}}{|\boldsymbol{r}_\eta|^3}\right)\frac{\boldsymbol{r}_\eta \times \boldsymbol{n}}{|\boldsymbol{r}_\eta|}, \tag{8}$$

where $\boldsymbol{r} \in S$ and we have omitted the asterisk for notational simplicity.

The specific form of the time evolution equation depends on the geometry of S. For example, if S is an infinite plane, we choose $\boldsymbol{r} = (x, y, 0)$ and $n = (0, 0, 1)$ so that

$$x_t = \left(c + \epsilon\frac{x_{\eta\eta}y_\eta - y_{\eta\eta}x_\eta}{(x_\eta^2 + y_\eta^2)^{\frac{3}{2}}}\right)\frac{y_\eta}{(x_\eta^2 + y_\eta^2)^{\frac{1}{2}}}, \tag{9}$$

$$y_t = \left(c + \epsilon\frac{x_{\eta\eta}y_\eta - y_{\eta\eta}x_\eta}{(x_\eta^2 + y_\eta^2)^{\frac{3}{2}}}\right)\frac{-x_\eta}{(x_\eta^2 + y_\eta^2)^{\frac{1}{2}}}. \tag{10}$$

These equations were given by Keener (1986) and used to analyse spiral wave boundaries arising from the Belousov–Zhabotinskii reaction (Keener 1986; Keener & Tyson 1986). In polar coordinates, they are

$$r_t = \left(c + \epsilon\frac{r\theta_\eta(r_{\eta\eta} - r\theta_\eta^2) - r_\eta(r\theta_{\eta\eta} + 2r_\eta\theta_\eta)}{(r_\eta^2 + r^2\theta_\eta^2)^{\frac{3}{2}}}\right)\frac{r\theta_\eta}{(r_\eta^2 + r^2\theta_\eta^2)^{\frac{1}{2}}}, \tag{11}$$

$$\theta_t = \left(c + \epsilon\frac{r\theta_\eta(r_{\eta\eta} - r\theta_\eta^2) - r_\eta(r\theta_{\eta\eta} + 2r_\eta\theta_\eta)}{(r_\eta^2 + r^2\theta_\eta^2)^{\frac{3}{2}}}\right)\frac{-r_\eta}{r(r_\eta^2 + r^2\theta_\eta^2)^{\frac{1}{2}}}. \tag{12}$$

If S is a sphere of unit radius we choose $\boldsymbol{r} = \boldsymbol{n} = \boldsymbol{e}$, where $|\boldsymbol{e}| = 1$ so that

$$\boldsymbol{e}_t = \left(c + \epsilon\frac{\boldsymbol{e}_{\eta\eta}\cdot\boldsymbol{e}_\eta \times \boldsymbol{e}}{|\boldsymbol{e}_\eta|^3}\right)\frac{\boldsymbol{e}_\eta \times \boldsymbol{e}}{|\boldsymbol{e}_\eta|}. \tag{13}$$

By use of this last equation, Grindrod & Gomatam (1987) were able to make

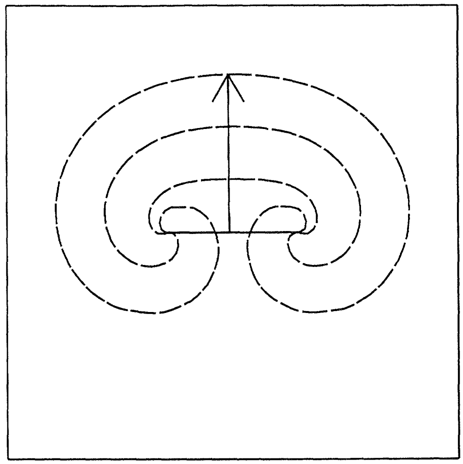

Figure 2. Temporal evolution of a spiral wave pattern. Numerical solution of (9), (10) on the infinite plane by an implicit second order finite difference scheme and fixed wave boundary end points results in the evolution of familiar spiral wave patterns ($c = 1.0$, $\epsilon = 0.1$). The location of the wave boundary at $t = 0$ is indicated by a solid line.

theoretical predictions for double spirals rotating on spheres, before the experimental discovery of them by Maselko & Showalter (1989).

3.1. *Zero-flux boundary conditions*

The symmetries of the asymptotic solutions for u and v along the wave boundary in the η-direction mean that when Neumann boundary conditions are imposed on the original reaction–diffusion system (1), the corresponding constraint on (8) is the orthogonal intersection of $\boldsymbol{r}_\eta$ with the domain boundary, $\partial\Omega$. It is evident that if such an intersection were non-orthogonal then the zero-flux boundary conditions would be violated at the point of intersection.

We define a scalar field g such that $\partial\Omega = \{\boldsymbol{r} \in S : g(\boldsymbol{r}) = 0\}$ where $\nabla g \neq 0$ when $g = 0$. Using g, the zero-flux boundary conditions can be written as

$$g(\boldsymbol{r}(0,t)) = 0, \tag{14}$$

$$\nabla g(\boldsymbol{r}(0,t)) \times \boldsymbol{r}_\eta(0,t) = 0, \tag{15}$$

where $\boldsymbol{r}_\eta$ intersects the boundary at $\eta = 0$ (figure 1). Note that the vector system (8) for waves propagating over surfaces is a pair of coupled second-order partial differential equations. Thus two conditions must be imposed at each end-point. Clearly, (15) is in agreement with this.

It is less clear what constraints to impose on each tip of an open wave boundary which does not approach the domain boundary. This is because the eikonal approximation is no longer valid at this interior wave boundary end-point; the concept of the curvature (κ) of the wave front makes little sense here. Zykov (1986) has shown that the behaviour depends on the local reaction kinetics in (1); tips remain essentially fixed for small ϵ, but begin to meander, in a small neighbourhood about the fixed point, as ϵ is increased. Meandering tips have been shown to move in small circles, sometimes with a secondary circular component, producing flower-like patterns (Lugosi 1989). The application of orthogonal (zero-flux) boundary conditions to small circular boundaries, excised from the solution domain at the wave tips, may emulate this meandering, at least when there is no secondary circular component. As ϵ decreases, the radius of these imaginary circular excisions is decreased, until the wave tips eventually become fixed. However, the wave tips are essentially stationary over long periods of time as they remain within a small neighbourhood of the fixed point. This leads us to suggest that by fixing the wave boundary end points, we retain the essential qualitative behaviour of the wave boundary movement.

4. Numerical solutions

The parametric form of the time-evolution equation for waves on surfaces (8) can be solved numerically by standard finite difference methods. This is facilitated by the fact that all the '$\delta\eta$' terms in the finite difference approximations for the η partial derivatives cancel. Thus we are conveniently precluded from explicitly stating the η-parametrization of the wave boundary. The discretization points chosen along the wave boundary at $t = 0$ define equal increments of η, and thereby the η-parametrization is defined for $t = 0$ (modulo a constant). The wave boundary movement is determined by the fact that points of fixed η are constrained to move perpendicularly to the wave boundary in the direction of μ ((3) an (4)). Thus the η-parametrization is defined for all time (modulo a constant), but is never given explicitly.

The application of a second-order implicit finite difference scheme to (9) and (10) yields a system of non-linear equations

$$\boldsymbol{F}(\boldsymbol{x}^n, \boldsymbol{x}^{n+1}, \boldsymbol{y}^n, \boldsymbol{y}^{n+1}; c, \epsilon) = 0,$$

where $\boldsymbol{x}^n$ and $\boldsymbol{y}^n$ give the coordinates of the wave boundary at time step n. The unknowns, $\boldsymbol{x}^{n+1}$ and $\boldsymbol{y}^{n+1}$, can be solved for by using Newton's Method at each time step. Figure 2 shows the temporal evolution of spiral wave patterns that result from solving the system (9) and (10) by this method while fixing the wave boundary end-points. The solution of the eikonal equation on a sphere (13) with fixed wave boundary end-points is shown in figure 3. Here, the secant method was used to solve the nonlinear system resulting from the application of a second order implicit finite difference scheme where $\boldsymbol{e} = (x, y, z)$ and $z = (1-x^2-y^2)^{\frac{1}{2}}$ with $0 \leqslant x^2+y^2 \leqslant 1$.

Numerical solution of the eikonal equation approximation (8) takes an order of magnitude less time than the numerical solution of the reaction–diffusion system (2); the CPU time to solve (9) and (10) was approximately 1/60 times the CPU time to solve (2), where the fast variable (u) had FitzHugh–Nagumo dynamics and explicit finite difference methods were used for both equations. The case tested was for a radially expanding wave boundary which was square at $t = 0$. Superimposition of the wave boundary predicted by (9) and (10) and the $u = 0.5$ contour given by (2) indicated a very close correlation for various ϵs. These results show that the numerical solution of the eikonal equation approximation is substantially faster and almost as accurate as the numerical solution of the reaction–diffusion system. However, further numerical comparisons of the accuracy are needed for various other reaction dynamics.

5. Geometric stability

Wave boundary solutions of the eikonal equation (5) which are stable as a family are referred to as being geometrically stable (Gomatam & Grindrod 1987). Geometric theory suggests that waves taking these forms may be stable solutions of the original

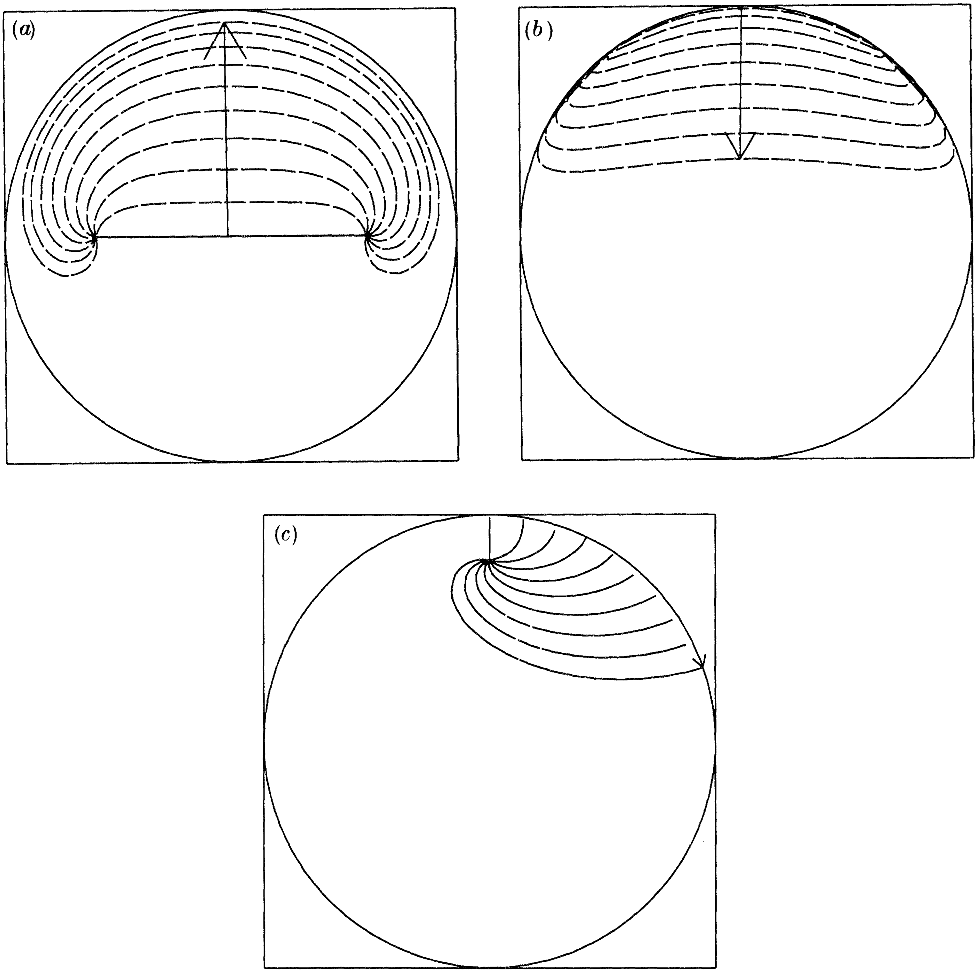

Figure 3. Solution of the eikonal equation on a unit sphere. Numerical solution of (13) by an implicit second-order finite difference scheme and fixed wave boundary end points yields the temporal evolution of spiral wave patterns on a sphere. (*a*) 'Birds-eye' view, (*b*) viewed from the front, (*c*) viewed from the right-hand side. ($c = 1.0$, $\epsilon = 0.1$).

reaction diffusion system (1). On the other hand, waves which are not geometrically stable are unlikely to be stable solutions of the original system, particularly in the limit of ϵ being very small.

Dispensing with the dummy coordinates η and λ helps in the analysis of geometric stability (although this simplification was not used in Gomatam & Grindrod (1987)). As in the three-dimensional case, this can be done when the wave boundary is expressible as a single-valued function. Suppose we consider a wave propagating over the infinite plane, and that for each t fixed, $y(\eta, t)$ is invertible with $y_\eta < 0$. In cartesian coordinates, $x(\eta, t) = X(y, t)$, so equations (9) and (10) yield

$$X_t = \epsilon \frac{X_{yy}}{(1+X_y^2)} + c(1+X_y^2)^{\frac{1}{2}}, \tag{16}$$

a simple quasi-linear evolution equation which is the two-dimensional analogue of

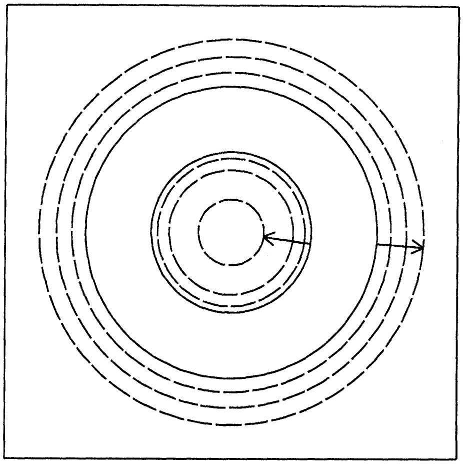

Figure 4. Threshold behaviour for radially expanding waves. Disturbances must exceed the critical radius $R_c = \epsilon/c$ to initiate a radially expanding wave. Numerical solutions of (9), (10), with $\epsilon/c = 0.5$, show how subthreshold disturbances ($R(0) = 0.44$) collapse while suprathreshold disturbances ($R(0) = 0.8$) initiate a radially expanding wave.

(7). The solution $X = ct$ represents a planar wave propagating over the (x, y)-plane in the x-direction. Linearizing about this solution by setting $X = ct + w(t, y)$ and keeping leading order terms yields

$$w_t = \epsilon w_{yy}.$$

These planar wave solutions are geometrically stable because $w \to 0$ uniformly as $t \to \infty$ provided $\int w(0, y)\,dy$ is finite.

We consider the use of polar coordinates. If, for each t fixed, $\theta(\eta, t)$ is invertible with $\theta_\eta > 0$, then by writing $r(\eta, t) = R(\theta, t)$, equations (11) and (12) yield

$$R_t = \epsilon \frac{(R_{\theta\theta} - 2R_\theta^2/R - R)}{(R_\theta^2 + R^2)} + c\frac{(R_\theta^2 + R^2)^{\frac{1}{2}}}{R}. \tag{17}$$

Simple solutions are obtained by assuming R is independent of θ and have the form

$$R_t = c - \epsilon/R(t). \tag{18}$$

Hence we obtain a spherical wave, centred at the origin, which exhibits threshold behaviour; disturbances must exceed a certain radius $R(0) > \epsilon/c$ to initiate a radially expanding wave (figure 4).

In Gomatam & Grindrod (1987) it was shown that (5) admits spherical waves in $\mathbb{R}^3$ which are geometrically stable. The same result can be obtained here for spherical waves in $\mathbb{R}^2$ by linearizing (17). Setting $R(t) = \rho(t) + s(t, \theta)$ and linearizing yields

$$s_z = s_{\theta\theta} + s, \tag{19}$$

where

$$z = \int_0^t \frac{\epsilon\,d\tau}{\rho^2(\tau)} \tag{20}$$

and $s(\theta) = s(2\pi + \theta)$. The solution $s = 0$ is unstable in the first eigenmode spanned by the function $\phi = 1$. However, the perturbation in this mode can be assumed to be zero if we permit the resetting of $\rho(0)$ so that $\int s(0, \theta)\,d\theta = 0$. The second eigen-mode spanned by the functions $\phi_1 = \cos(\theta)$ and $\phi_2 = \sin(\theta)$ is neutrally stable. The perturbation in this mode can also be assumed to be zero if we allow a shift in the

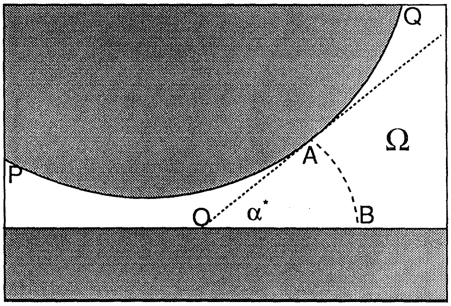

Figure 5. The domain, Ω, for analysis of stable stationary waves. Here, $\partial\Omega$ is given by $\theta = 0$ (below) and $g(r, \theta) = 0$ (above). The wave boundary is depicted by the arc of a circle with radius ϵ/c, centred at the point O. Thus, in the polar coordinate system, $A = (\epsilon/c, \alpha^*)$ and $B = (\epsilon/c, 0)$.

origin of the spherical wave so that $\int s(0,\theta) \sin(\theta)\,\mathrm{d}\theta = 0$ and $\int s(0,\theta)\cos(\theta)\,\mathrm{d}\theta = 0$. The origin for (19) is stable in the higher eigen-modes ($\geqslant 2$). Thus the three-parameter family of spherical waves defined by an arbitrary initial radius and origin shift is stable.

5.1. *Stable stationary waves*

We consider stationary waves that satisfy (5) in the plane. By definition $N \equiv 0$, so such waves have constant curvature and must lie in arcs of circles of radius ϵ/c. Here the rest point, $r = \epsilon/c$ is unstable in the first eigen-mode as we do not allow an arbitrary resetting of the initial radius. However, by considering some simple problems involving bounded domains we shall show that geometrically stable stationary waves are possible.

Consider a wave propagating through the domain $\Omega \subset \mathbb{R}^2$ shown in figure 5. The curve AB represents the wave boundary for an excitable system with zero-flux boundary conditions, and is depicted by the arc of a circle with the radius ϵ/c, centred at the point O. We introduce the polar coordinates (r, θ) centred at the origin O, thereby making $A = (\epsilon/c, \alpha^*)$. We assume that the boundary curve PAQ is given by $g(r, \eta) = 0$ for some smooth function g, with a non-vanishing gradient in the neighbourhood of A. We write (8) in polar coordinates with $r = r(\theta, t)$. Thus perturbations of this stationary wave must satisfy

$$r_t = \epsilon\frac{(r_{\theta\theta} - 2r_\theta^2/r - r)}{(r_\theta^2 + r^2)} + c\frac{(r_\theta^2 + r^2)^{\frac{1}{2}}}{r}, \tag{21}$$

for $0 \leqslant \theta \leqslant \alpha$ and $t \geqslant 0$, together with the boundary conditions

$$g = 0, \tag{22}$$

$$r^2 g_r = r_\theta g_\theta, \tag{23}$$

at $(r, \theta) = (r(\alpha, t), \alpha)$ and

$$r_\theta = 0 \tag{24}$$

at $\theta = 0$.

The conditions (22)–(24) ensure that the wave boundary meets $\partial\Omega$ orthogonally at the points A and B. Thus (21)–(24) represents a moving boundary problem with $\alpha(t)$ being dependent on the solution r.

Perturbing the stationary wave solution, $(r, \theta) = (\epsilon/c, \alpha^*)$ to

$$(r, \theta) = (\epsilon/c + s(t, \theta), \alpha^* + \beta)$$

and linearizing (21)–(24) yields

$$s_t = (s_{\theta\theta}+s)(c^2/\epsilon) \tag{25}$$

for $0 \leqslant \theta \leqslant \alpha^*$ and $t \geqslant 0$ together with the boundary conditions

$$g_r s + g_\theta \beta = 0, \tag{26}$$

$$(\epsilon^2/c^2)(g_{rr} s + g_{r\theta}\beta) = s_\theta g_\theta \tag{27}$$

at $(r,\theta) = (\epsilon/c, \alpha^*)$ and

$$s_\theta = 0 \tag{28}$$

at $\theta = 0$. However, $g_r(\epsilon/c, \alpha^*) = 0$ means that $\beta = 0$ by (26). Thus (27) becomes

$$(\epsilon^2/c^2)(g_{rr}/g_\theta)\, s = s_\theta \tag{29}$$

at $(r,\theta) = (\epsilon/c, \alpha^*)$.

Eigenfunctions of the resulting stability problem defined by (25), (28) and (29) are of the form

$$s = \exp\left((1-\lambda^2)\,\epsilon t/c^2\right) \cos \lambda\theta, \tag{30}$$

where λ is real, non-negative, and satisfies

$$-\lambda \tan \lambda\alpha^* = (\epsilon^2/c^2)(g_{rr}/g_\theta)$$

at $(r,\theta) = (\epsilon/c, \alpha^*)$. Thus for stability we require that $\lambda > 1$ in (30), which is true for $0 < \alpha^* < \frac{1}{2}\pi$ if and only if

$$(\epsilon^2/c^2)(g_{rr}/g_\theta) \notin [-\tan(\alpha^*), 0] \tag{31}$$

at $(r,\theta) = (\epsilon/c, \alpha^*)$.

By choosing

$$g(r,\theta) = y - h(x),$$

with $h'(x) > 0$ (see figure 5) we can put the stability criterion (31) in a simpler form. Note that the origin in these (x, y) coordinates is not necessarily coincident with our origin, O, introduced for the polar coordinates. If the x-coordinate of A is x^*, then the stationary wave solution is given by

$$h'(x^*) = \tan(\alpha^*)$$

and

$$h(x^*) = (\epsilon/c)\sin(\alpha^*) = (\epsilon/c)\frac{h'(x^*)}{(1+h'^2(x^*))^{\frac{1}{2}}}. \tag{32}$$

The stability criterion (31) now becomes

$$h'' \notin [0, (c/\epsilon)\, h'(1+h'^2)^{\frac{3}{2}}] \tag{33}$$

at $x = x^*$. For concave domains, such as the one shown in figure 5, we have $h''(x^*) > 0$. Thus if $h''(x^*)$ is large enough, the wave is stable.

By way of an example, we consider the case where the curve PQ in figure 5 is given by the arc of a circle with radius ρ. Here

$$h(x) = \delta + \rho - (\rho^2 - x^2)^{\frac{1}{2}}$$

and $0 < x < \rho$. By using (32) we see that there are two standing wave solutions for

$$\epsilon > \epsilon_c = c\,(\delta(\delta + 2\rho))^{\frac{1}{2}} \tag{34}$$

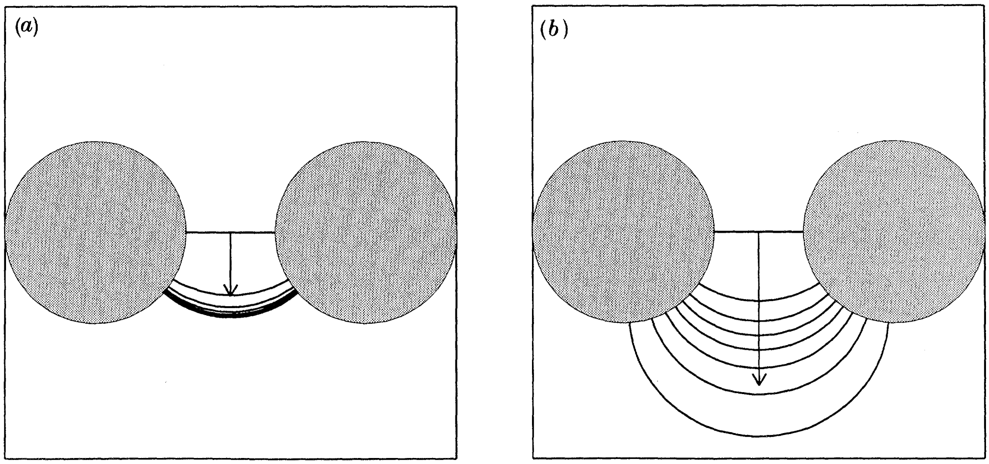

Figure 6. Geometrically stable standing wave. Numerical solution of (9), (10) with orthogonal boundary conditions on a non-convex domain reveals a geometrically stable wave for $\epsilon > \epsilon_c$. Here, the solution domain is the infinite plane, with two circular excisions of radius ρ which are separated by the distance 2δ. By choosing $\rho = 2\delta$ and $c = 1$ we have $\epsilon_c = \delta\sqrt{5}$ (34). A geometrically stable standing wave results when $\epsilon = 2.3\delta > \epsilon_c$ (a). This standing solution disappears when $\epsilon = 2.1\delta < \epsilon_c$ (b).

which coalesce and then disappear at

$$x^* = x_c = \rho(\delta(\delta+2\rho))^{\frac{1}{2}}/(\delta+\rho)$$

as ϵ passes through ϵ_c. The stability criterion (33) indicates that the inner standing wave is locally stable while the outer standing wave is unstable. Thus if a wave is initiated in the domain

$$\Omega = \{x \geqslant 0 \quad \text{and} \quad 0 \leqslant y \leqslant \delta+\rho-(\rho^2-x^2)^{\frac{1}{2}}\}$$

at $x = 0, 0 \leqslant y \leqslant \delta$, it tends towards the stationary wave $x^* = x_c$ provided $\epsilon > \epsilon_c$. The behaviour for ϵ less than and greater than ϵ_c is numerically simulated in figure 6.

Having demonstrated one possible situation where a standing wave is stable, we forego the opportunity to construct more elaborate examples and briefly focus on the consequences of such behaviour. The point to note is that reaction–diffusion waves cannot propagate out of thin slits. Figure 7 shows the stable stationary steady state configuration assumed by a planar travelling wave as it exits from a narrow slit into a larger reservoir. In this numerical simulation we solved the bistable reaction–diffusion system with cubic dynamics, given by

$$\epsilon u_t = \epsilon^2 \Delta u + u(1-u)(u-a). \tag{35}$$

while applying zero-flux conditions at the domain boundary. Thus the rest state of the reaction–diffusion system is numerically shown to exist as a stable configuration, which is what the geometric theory predicts.

6. Discussion

We have demonstrated stability behaviour, threshold results and stationary waves for the eikonal equation approximation (5). We have shown that this approximation can be solved numerically, yielding a significant computational advantage over

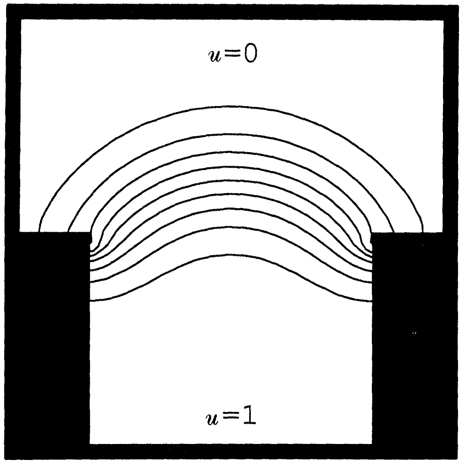

Figure 7. The rest state of a bistable reaction–diffusion system is shown to exist as a stable configuration. The numerical solution of (35) with zero-flux boundary conditions by finite difference methods reveals a stable stationary configuration as the wave is exiting from the mouth of the channel. Here, the channel width is 1.0 and $\epsilon = 0.08$, while $a = 0.4$ yields an effective planar travelling wave speed of $c = \sqrt{2}(1/2-0.4) = 0.1414$. Isoclines are shown for 0.1 increments of u.

solving the original reaction–diffusion equation. There is also an important conceptual advantage to be gained by working with the eikonal equation; modellers can understand the concepts of threshold behaviour and stationary waves with an insight which is not afforded by consideration of the original reaction–diffusion system (1). We hope that this will encourage more experimental and theoretical work in a number of areas which previously were held back by the complexity or intractability of large systems of excitable reaction–diffusion equations.

Our analysis of the stationary waves, arising from an excitable system with Neumann boundary conditions on a non-convex domain, suggests new experimental situations which may yield stationary waves. For example, by placing two impervious disks adjacent to each other in reagent, one could emulate a small slit which should block a wave of excitation in the Belousov–Zhabotinskii reaction. Alternatively, applications to the theory of neuromuscular systems may lead to a better understanding of the underlying causes of abnormalities such as one-way blocks in cardiac tissue (Lewis & Grindrod 1991).

This work (J.D.M.) was supported in part by a Grant (DMS-8902878) from the U.S. National Science Foundation.

References

FitzHugh, R. 1961 Impulses and physiological states in theoretical models of nerve membrane. *Biophys. J.* **1**, 445–466.

Gomatam, J. & Grindrod, P. 1987 Three-dimensional waves in excitable reaction–diffusion systems. *J. math. Biol.* **25**, 611–622.

Gorelova, N. A. & Bŭres, J. 1983 Spiral waves of spreading depression in the isolated chicken retina. *J. Neurobiol.* **14**, 353–363.

Grindrod, P. 1991 *Patterns and waves in reaction diffusion*. Oxford University Press. (In the press.)

Grindrod, P. & Gomatam, J. 1987 The geometry and motion of reaction-diffusion waves on closed two-dimensional manifolds. *J. math. Biol.* **25**, 597–610.

Hodgkin, A. L. & Huxley, A. F. 1952 A quantitative description of membrane current and its application to conduction and excitation in nerve. *J. Physiol.* **117**, 500–544.

Keener, J. P. 1986 A geometrical theory for spiral waves in excitable media. *SIAM J. appl. Math.* **46**, 1039–1056.

Keener, J. P. & Tyson, J. J. 1986 Spiral waves in the Belousov–Zhabotinskii reaction. *Physica* D **21**, 307–324.

Lewis, M. A. & Grindrod, P. 1991 One-way blocks in cardiac tissue: A mechanism for propagation failure in Purkinje fibres. *Bull. Math. Biol.* (In the press.)

Lugosi, E. 1989 Analysis of meandering in Zykov kinetics. *Physica* D **40**, 331–337.

Maselko, J. & Showalter, K. 1989 Chemical waves on spherical surfaces. *Nature, Lond.* **3339**, 609–611.

Matano, H. 1979 Asymptotic behaviour and stability of solutions of semi-linear diffusion equations. *Publ. Res. Inst. Math. Sci.* **15**, 401–454.

Miura, R. M. & Plant, R. E. 1981 Rotating waves in models of excitable media. In *Differential equations and applications in ecology, epidemics, and population problems* (ed. S. N. Busenberg & K. L. Cooke), pp. 247–257. New York: Academic Press.

Murray, J. D. 1989 *Mathematical biology*. Heidelberg: Springer Verlag.

Nagumo, J., Arimoto, S. & Yoshizawa, S. 1962 An active pulse transmission line simulating nerve axon. *Proc. IRE*. **50**, 2061–2070.

Shibata, M. & Bŭres, J. 1974 Optimum topographical conditions for reverberating cortical spreading in rats. *J. Neurobiol.* **5**, 107–118.

Tyson, J. J., Alexander, K. A., Manoranjan, V. S. & Murray, J. D. 1989 Spiral waves of cyclic amp in a model of slime mold aggregation. *Physica* D **34**, 193–207.

Tyson, J. J. & Murray, J. D. 1989 Cyclic AMP waves during aggregation of Dictyostelium amoebae. *Development* **106**, 421–426.

Winfree, A. T. 1987 *When time breaks down: the three-dimensional dynamics of electrochemical waves and cardiac arrhythmias*. Princeton University Press.

Zykov, V. S. 1986 Cycloidal circulation of spiral waves in an excitable medium. *Biophys.* **31**, 940–944.

Zykov, V. S. 1987 *Simulation of wave processes in excitable media*. (ed. A. T. Winfree). Manchester University Press.

Received 20 August 1990; accepted 16 October 1990